



# Time-Temperature-Precipitation Behavior in Al-Li Alloy 2195

*P.S. Chen*

*IIT Research Institute, Huntsville, Alabama*

*B.N. Bhat*

*Marshall Space Flight Center, Marshall Space Flight Center, Alabama*



## The NASA STI Program Office...in Profile

Since its founding, NASA has been dedicated to the advancement of aeronautics and space science. The NASA Scientific and Technical Information (STI) Program Office plays a key part in helping NASA maintain this important role.

The NASA STI Program Office is operated by Langley Research Center, the lead center for NASA's scientific and technical information. The NASA STI Program Office provides access to the NASA STI Database, the largest collection of aeronautical and space science STI in the world. The Program Office is also NASA's institutional mechanism for disseminating the results of its research and development activities. These results are published by NASA in the NASA STI Report Series, which includes the following report types:

- **TECHNICAL PUBLICATION.** Reports of completed research or a major significant phase of research that present the results of NASA programs and include extensive data or theoretical analysis. Includes compilations of significant scientific and technical data and information deemed to be of continuing reference value. NASA's counterpart of peer-reviewed formal professional papers but has less stringent limitations on manuscript length and extent of graphic presentations.
- **TECHNICAL MEMORANDUM.** Scientific and technical findings that are preliminary or of specialized interest, e.g., quick release reports, working papers, and bibliographies that contain minimal annotation. Does not contain extensive analysis.
- **CONTRACTOR REPORT.** Scientific and technical findings by NASA-sponsored contractors and grantees.
- **CONFERENCE PUBLICATION.** Collected papers from scientific and technical conferences, symposia, seminars, or other meetings sponsored or cosponsored by NASA.
- **SPECIAL PUBLICATION.** Scientific, technical, or historical information from NASA programs, projects, and mission, often concerned with subjects having substantial public interest.
- **TECHNICAL TRANSLATION.** English-language translations of foreign scientific and technical material pertinent to NASA's mission.

Specialized services that complement the STI Program Office's diverse offerings include creating custom thesauri, building customized databases, organizing and publishing research results...even providing videos.

For more information about the NASA STI Program Office, see the following:

- Access the NASA STI Program Home Page at <http://www.sti.nasa.gov>
- E-mail your question via the Internet to [help@sti.nasa.gov](mailto:help@sti.nasa.gov)
- Fax your question to the NASA Access Help Desk at (301) 621-0134
- Telephone the NASA Access Help Desk at (301) 621-0390
- Write to:  
NASA Access Help Desk  
NASA Center for AeroSpace Information  
7121 Standard Drive  
Hanover, MD 21076-1320



# **Time-Temperature-Precipitation Behavior in Al-Li Alloy 2195**

*P.S. Chen*

*IIT Research Institute, Huntsville, Alabama*

*B.N. Bhat*

*Marshall Space Flight Center, Marshall Space Flight Center, Alabama*

National Aeronautics and  
Space Administration

Marshall Space Flight Center • MSFC, Alabama 35812

---

***February 2002***

Available from:

NASA Center for AeroSpace Information  
7121 Standard Drive  
Hanover, MD 21076-1320  
(301) 621-0390

National Technical Information Service  
5285 Port Royal Road  
Springfield, VA 22161  
(703) 487-4650

## TABLE OF CONTENTS

1. INTRODUCTION .....	1
2. TECHNICAL APPROACH .....	2
3. EXPERIMENTAL PROCEDURES .....	3
3.1 Processing .....	3
3.2 Microstructural Characterization .....	3
4. RESULTS AND DISCUSSION.....	4
4.1 <i>GP</i> Zone, $\theta''$ ( $\text{Al}_2\text{Cu}$ ), and $\delta'$ ( $\text{Al}_3\text{Zr}$ ) .....	4
4.2 $T_1$ ( $\text{Al}_2\text{CuLi}$ ).....	5
4.3 $\theta'$ ( $\text{Al}_2\text{Cu}$ ) and $\theta$ ( $\text{Al}_2\text{Cu}$ ) .....	6
4.4 $T_2$ ( $\text{Al}_5\text{Li}_3\text{Cu}$ ) and $T_B$ ( $\text{Al}_{7.5}\text{LiCu}_4$ ) .....	7
4.5 Time-Temperature-Precipitation Diagrams .....	8
5. SUMMARY .....	11
REFERENCES .....	13

## LIST OF FIGURES

1.	Heat-treatment matrix for solution-treated Al-Li 2195 .....	3
2.	Hardness variations as a function of heat-treatment conditions .....	4
3.	Matrix consisting of entangled dislocations and dispersed $\delta'$ particles after aging at 200 °F/1 hr (dissolved <i>GP</i> zone and $\theta''$ due to reversion) .....	5
4.	$T_1$ nucleation occurring preferentially at subgrain boundaries at 300 °F .....	5
5.	(a) Subgrain boundary $T_1$ , which grew longer and thicker than matrix $T_1$ , and (b) significant occurrence of nucleation and growth of $T_1$ .....	6
6.	Microstructure primarily consisting of matrix $\theta'$ and grain boundary $\theta$ after heat treatment at 700 °F/1 hr .....	6
7.	$\theta'$ nucleation diminishing significantly at 800 °F .....	7
8.	$T_2$ and $T_B$ forming at 800 °F/0.1 hr .....	7
9.	TTP diagrams for Al-Li 2195 .....	8
10.	Enhanced $\theta''$ and $T_1$ nucleation in the matrix (rather than at subgrain boundaries) during the first step of TS aging (270 °F/20 hr) .....	9
11.	(a) No $T_1$ precipitation seen at subgrain boundaries after TS aging as compared to (b) preferential $T_1$ precipitation seen at subgrain boundaries after conventional aging .....	10
12.	Significantly enhanced CFT of Al-Li 2195 after TS aging .....	10

## LIST OF ACRONYMS AND SYMBOLS

$\delta'$	Al <sub>3</sub> Li precipitate compound
$\theta, \theta', \theta''$	Al <sub>2</sub> Cu precipitate compounds
Ag	silver
Al	aluminum
CFT	cryogenic fracture toughness
Cu	copper
<i>GP</i> zone	Guinier-Preston zone
HAZ	heat-affected zone
HR <sub>B</sub>	Rockwell hardness B scale
Li	lithium
Mg	magnesium
SLWT	super lightweight tank
$T_1$	Al <sub>2</sub> CuLi strengthening precipitate
$T_2$	Al <sub>5</sub> Li <sub>3</sub> Cu strengthening precipitate
$T_B$	Al <sub>7.5</sub> LiCu <sub>4</sub> strengthening precipitate
TEM	transmission electron microscopy
TS	two step
TTP	time-temperature-precipitation
Zr	zirconium

## TECHNICAL MEMORANDUM

### TIME-TEMPERATURE-PRECIPIATION BEHAVIOR IN AL-LI ALLOY 2195

#### 1. INTRODUCTION

Transmission electron microscopy (TEM) was used to study time-temperature-precipitation (TTP) behavior in aluminum-lithium (Al-Li) 2195 alloy. Al-Li 2195 (nominally Al + 4 percent Cu + 1 percent Li + 0.3 percent Ag + 0.3 percent Mg + 0.1 percent Zr) was initially solutionized for 1 hr at 950 °F and then stretched 3 percent. Heat treatments were conducted for up to 100 hr at temperatures ranging from 200 to 1,000 °F. TTP diagrams were determined for both matrix and subgrain boundaries. Depending upon heat treatment conditions, precipitate phases (such as Guinier-Preston (*GP*) zone,  $\theta''$ ,  $\theta'$ ,  $\theta$ ,  $\delta'$ ,  $T_1$ ,  $T_B$ , and  $T_2$ ) were found in the alloy. The TTP diagrams were applied as a guide to avoid  $T_1$  precipitation at subgrain boundaries, as part of an effort to improve the alloy's cryogenic fracture toughness (CFT). New understanding of TTP behavior was instrumental in the development of a two-step (TS) artificial aging treatment that significantly enhances CFT in Al-Li 2195.

## 2. TECHNICAL APPROACH

Due to its low density, high modulus, and good cryogenic properties, Al-Li 2195 was selected as the main structural alloy for the Space Shuttle's external super lightweight tank (SLWT).<sup>1,2</sup> Al-Li 2195 has significantly higher strength than conventional 2xxx alloys (such as Al 2219) at both ambient and cryogenic temperatures, and it can be strengthened further through the use of an aging treatment that precipitates the primary strengthening precipitate  $T_1$  ( $\text{Al}_2\text{CuLi}$ ). Other phases (such as  $GP$  zone,  $\theta''$ ,  $\theta'$ ,  $\theta$ , and  $\delta'$ ) are present after the alloy is artificially aged. Some work has been done on the precipitation characteristics of  $T_1$  in order to optimize materials strength and fracture toughness.<sup>3</sup> However, no systematic study on TTP behavior had previously been undertaken.

TTP behavior was studied at temperatures  $<400$  °F, in part because a recent study<sup>1,2</sup> had indicated that CFT is related to the density, size, and location of  $T_1$ . CFT decreases considerably as  $T_1$  increases in density at the subgrain boundaries, but such precipitation could perhaps be minimized by an advanced aging treatment based upon a better understanding of TTP behavior in Al-Li 2195. TTP was also studied at higher temperatures, due to the importance of alloy properties in the heat-affected zone (HAZ), which is subjected to thermal cycles during weld repair. Since any additional thermal cycles will affect precipitate stability and transformation of the structural alloy, TTP diagrams must be available for comparison to welded microstructures in order to understand the thermal history of each SLWT.

This study was conducted to develop TTP diagrams for solution-treated and stretched Al-Li 2195, which will allow its precipitation reactions to be predicted at any aging temperature. Such diagrams will serve as a guide to optimize the alloy's mechanical properties by varying heat treatment parameters. This understanding will assist in the development of welding parameters to further improve the mechanical properties of Al-Li 2195 for use in SLWT applications.

### 3. EXPERIMENTAL PROCEDURES

#### 3.1 Processing

The alloy (nominally Al-4.19Cu-0.95Li-0.29Mg-0.31Ag-0.12Zr) used in this study was processed by Reynolds and supplied in the form of 1.7-in-thick rolled plates. Rolling was conducted on an initial ingot thickness of  $\approx 13$  in, in the temperature range of 700 to 800 °F. The plates were then given a solutionizing treatment for 1 hr at 950 °F and then stretched 3 percent at ambient temperature. After stretching, the specimens were heat treated in the time-temperature envelope of 0.1 to 100 hr at 200 to 1,000 °F (see fig. 1). After heat treatment, hardness was measured for each specimen using the Rockwell hardness B scale ( $HR_B$ ).

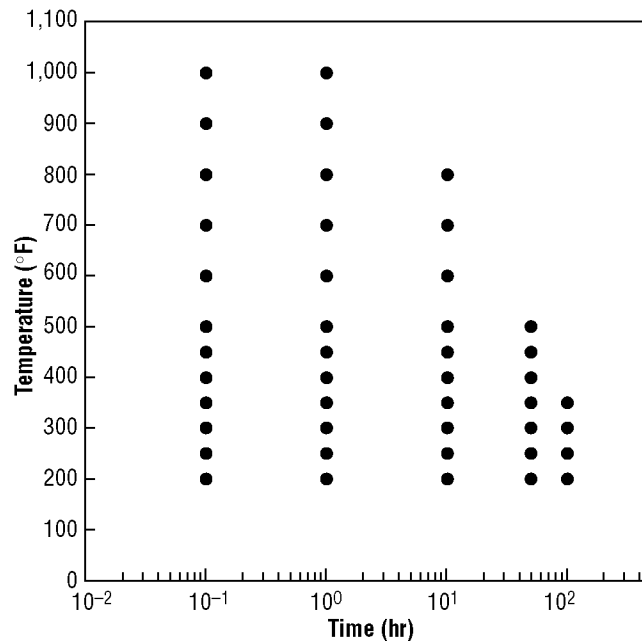


Figure 1. Heat-treatment matrix for solution-treated Al-Li 2195.

#### 3.2 Microstructural Characterization

Specimens were sliced from the plates and mechanically ground to the desired thickness for microstructural examination, which was carried out using a JEOL, Ltd. 2000F transmission electron microscope operated at 200 kV. Samples were twinjet electropolished to perforation at  $-20$  °F and 12 V in an electrolyte of 30-percent nitric acid in methanol. Precipitates were examined by the combined use of selected area diffraction and bright field/dark field techniques. Matrix and subgrain boundary precipitates were examined using an electron beam direction near the  $[110]_{\text{matrix}}$  zone axis.

## 4. RESULTS AND DISCUSSION

The Al-Li 2195 plate had a predominantly unrecrystallized microstructure, with coarse and pancake-shaped grains elongated along the rolling direction. The as-solution-treated and stretched microstructure primarily contained *GP* zone (localized concentrations of Cu atoms) due to natural aging,<sup>5</sup> but was free of other secondary phases. Depending on heat-treatment conditions, the solution-treated material can decompose and precipitate via several different reactions. Therefore, hardness can vary as a function of heat-treatment conditions (see fig. 2).

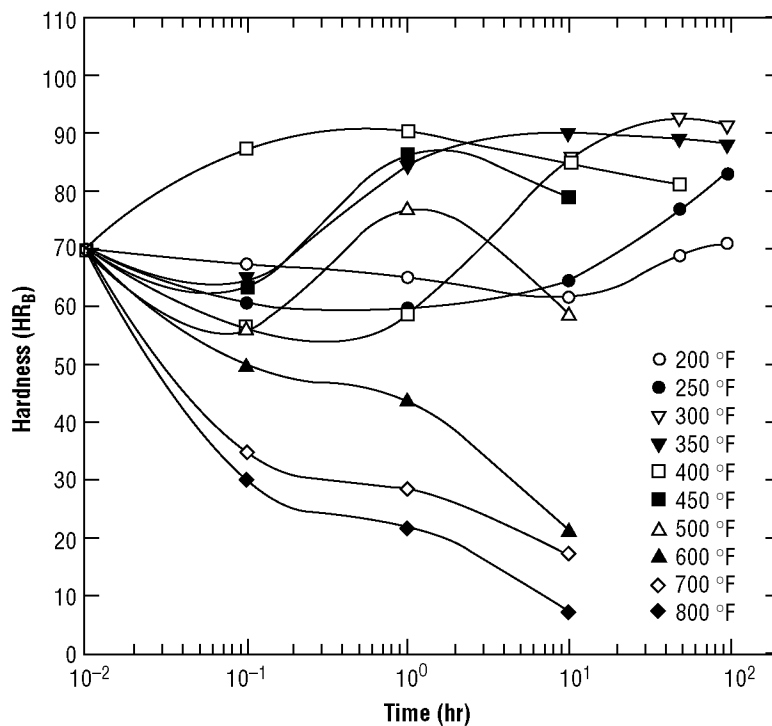


Figure 2. Hardness variations as a function of heat-treatment conditions.

### 4.1 *GP* Zone, $\theta''$ ( $\text{Al}_2\text{Cu}$ ), and $\delta'$ ( $\text{Al}_3\text{Zr}$ )

*GP* zone,  $\theta''$ , and  $\delta'$  were the primary precipitate phases at 200 and 250 °F. During early stages of heat treatment (<500 °F), reversion caused a sharp decrease in hardness<sup>5</sup> associated with some dissolution of *GP* zones and  $\delta'$ . At 200 and 250 °F, the matrix microstructure consisted of primary entangled dislocations and dispersed  $\delta'$  particles. No sign of  $T_1$  nucleation was found under these conditions (see fig. 3). After longer heat treatment at 250 °F, a slight increase in hardness was noted, due to continual growth of  $\theta''$ .

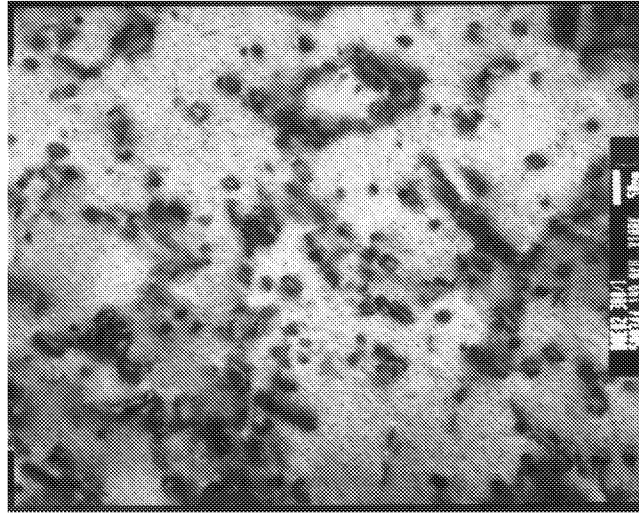


Figure 3. Matrix consisting of entangled dislocations and dispersed  $\delta'$  particles after aging at 200 °F/1 hr (dissolved  $GP$  zone and  $\theta''$  due to reversion).

#### 4.2 $T_1$ ( $Al_2CuLi$ )

$T_1$  was the predominant precipitate at temperatures ranging from 280 to 500 °F. With its plate-shaped morphology,  $T_1$  is the primary phase responsible for the increased hardness at temperatures <500 °F. It has a very strong tendency to nucleate at subgrain boundaries and grow very rapidly there (see fig. 4) in the same temperature range as  $T_1$  formed in the matrix. However, subgrain  $T_1$  is usually thicker, shorter, and has a smaller diameter than matrix  $T_1$ . Only when the habit plane of  $T_1$  was nearly parallel to the subgrain boundary plane did the precipitate grow very long (see fig. 5). In the matrix,  $T_1$  grew continuously at the expense of  $GP$  zones,  $\theta'$ , and  $\theta''$ . Exposure for a short time (6 min) at 350 and 400 °F led to abundant nucleation and significant coarsening of  $T_1$  (see fig. 6).

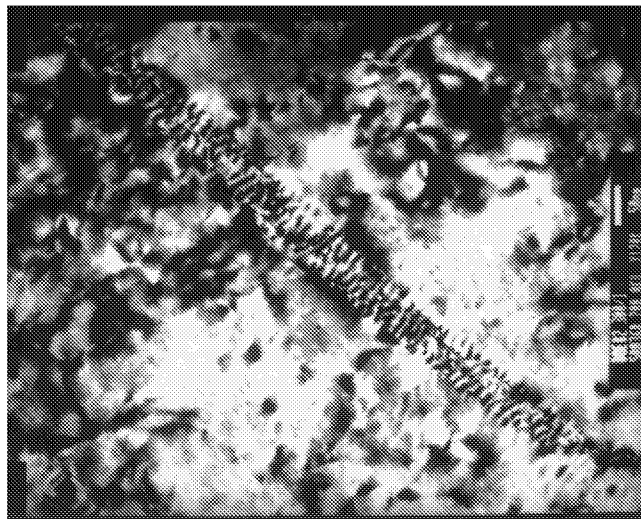
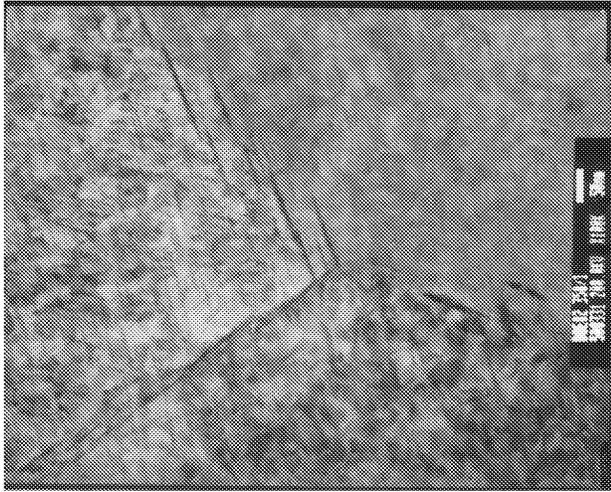


Figure 4.  $T_1$  nucleation occurring preferentially at subgrain boundaries at 300 °F.



(a) At 350 °F/0.1 hr



(b) At 400 °F/0.1 hr

Figure 5. (a) Subgrain boundary  $T_1$ , which grew longer and thicker than matrix  $T_1$ , and (b) significant occurrence of nucleation and growth of  $T_1$ .

#### 4.3 $\theta'$ ( $\text{Al}_2\text{Cu}$ ) and $\theta$ ( $\text{Al}_2\text{Cu}$ )

In the early stages of heat treatment at elevated temperatures (600 to 700 °F),  $\theta'$  became the dominant precipitate (see fig. 6). Prolonged exposure at 700 °F led to the precipitation of equilibrium phases  $\theta$  in the matrix and grain boundaries. Above 800 °F, the formation of incoherent  $\theta$  accompanied the recovery and recrystallization processes, as evidenced by increased dislocation pileup and grain growth. At 800 °F,  $\theta'$  nucleation diminished significantly (see fig. 7).

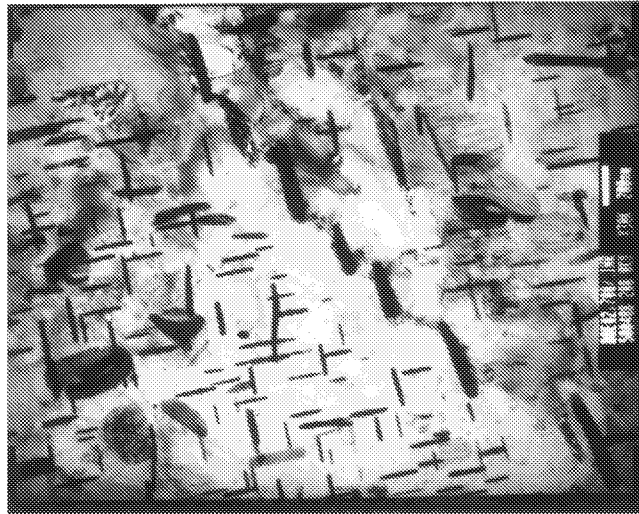


Figure 6. Microstructure primarily consisting of matrix  $\theta'$  and grain boundary  $\theta$  after heat treatment at 700 °F/1 hr.

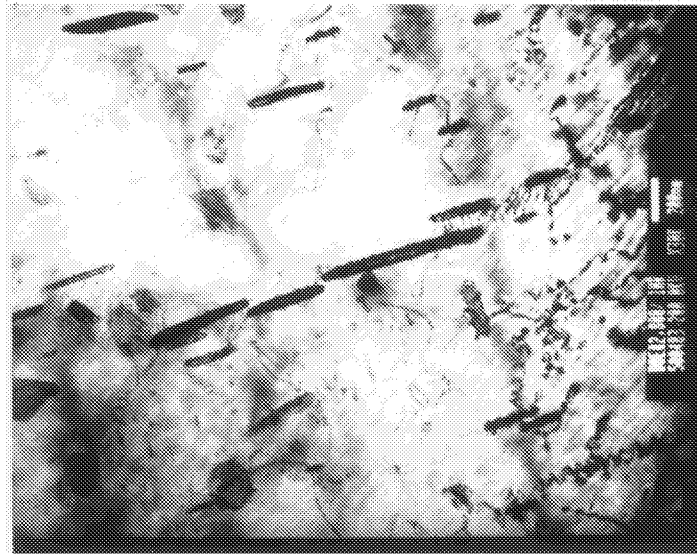


Figure 7.  $\theta'$  nucleation diminishing significantly at 800 °F.

#### 4.4 $T_2$ ( $\text{Al}_5\text{Li}_3\text{Cu}$ ) and $T_B$ ( $\text{Al}_{7.5}\text{LiCu}_4$ )

$\theta'$ ,  $\theta$ ,  $T_2$ , and  $T_B$  formed in the matrix and subgrain boundaries after 10 hr at 700 and 800 °F. Prolonged exposure at 800 °F led to the precipitation of equilibrium phases  $T_B$  (primarily in the matrix and grain boundaries) and  $T_2$  (primarily at grain boundaries).  $T_B$  precipitated in the matrix and appeared to grow at the expense of  $\theta'$  and  $\theta$ , whereas  $T_2$  led to continuous grain boundary coverage by coexisting with  $\theta$  at grain boundaries (see fig. 8).

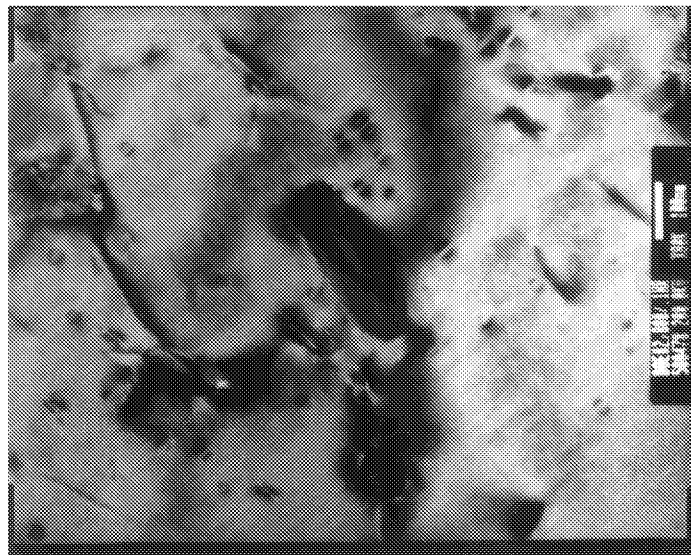


Figure 8.  $T_2$  and  $T_B$  forming at 800 °F/0.1 hr.

At temperatures  $>600$  °F, a significant drop in hardness occurred, which can be explained by insufficient nucleation of  $T_1$  and precipitation of incoherent equilibrium phases  $\theta$ ,  $T_B$ , and  $T_2$ . The number of subgrains also diminished due to extensive recovery and early stage of recrystallization. At temperatures  $>900$  °F, more significant recrystallization and grain growth occurred, creating a microstructure essentially devoid of any strengthening precipitates in both the matrix and grain boundaries.

#### 4.5 Time-Temperature-Precipitation Diagrams

The TTP diagrams consisted of C-curves for  $T_1$ ,  $\theta'$ ,  $\theta''$ ,  $\theta$ ,  $T_2$ , and  $T_B$  in the matrix and  $T_1$ ,  $\theta'$ ,  $\theta$ ,  $T_2$ , and  $T_B$  at subgrain boundaries (see fig. 9). The phase boundaries (estimated by curve-fitting approach from TEM observation of the experimental samples) are given only for the start of each precipitation, and completion curves were not determined. Therefore, the region to the right of a curve represents the time-temperature envelope for which that phase was present in the microstructure after heat treatment.

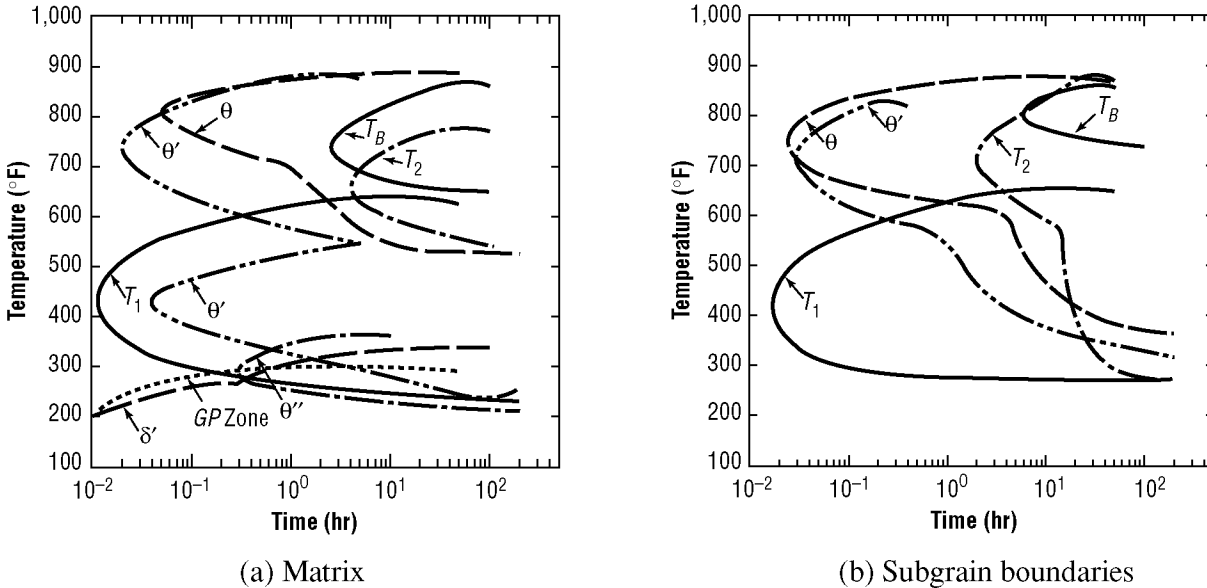


Figure 9. TTP diagrams for Al-Li 2195.

A very short but finite nucleation time ( $<6$  min) exists for the onset of  $T_1$  precipitation. In most cases, subgrain boundaries are favorable nucleation sites for  $T_1$  at temperatures ranging from  $\approx 280$  to  $500$  °F. Nucleation of  $T_1$  is very rapid and, once nucleated, subgrain boundary  $T_1$  always grows faster than matrix  $T_1$ . The only ways found to avoid preferential  $T_1$  precipitation at subgrain boundaries were to age the material  $<280$  °F (the temperature at which  $T_1$  forms) or enhance  $T_1$  nucleation and growth in the matrix so that  $T_1$ -forming elements (such as Li and Cu) became depleted at subgrain boundaries.

Caution should be exercised when using TTP diagrams for Al-Li 2195, since the energy state (e.g., grain size, hot working history, solution treatment temperature, degree of stretch) can shift relationships to the left or right. The commercial solution heat treatment commonly used for Al-Li 2195 ( $950$  °F) would be expected to result in complete dissolution of all phases.

Although precipitation behavior may be affected by composition variations from heat to heat, these TTP diagrams can be used as a guide to select appropriate heat treatments for different service applications. If high strength and high fracture toughness are needed, then aging treatments should be selected from diagrams which precipitate maximum matrix  $T_1$  for strength while avoiding or minimizing precipitation of subgrain boundary  $T_1$ .

CFT and cryogenic strength are considered critical for the SLWT (which houses liquid oxygen and liquid hydrogen), as is the need for higher strength and fracture toughness at cryogenic temperatures than at ambient temperature (in order to avoid expensive cryogenic proof testing). Unfortunately, some commercial 2195 material was disqualified from the SLWT program when it exhibited unexpectedly low CFT which proved to be related to the density, size, and location of  $T_1$ .<sup>1,2</sup> Attempts were made to improve the fracture toughness of such material by reducing subgrain boundary  $T_1$  while enhancing the nucleation of matrix  $T_1$ , based on the observation that CFT decreases considerably as  $T_1$  increases in density at the subgrain boundaries.

Since the TTP diagrams indicate that  $T_1$  nucleation and growth can be controlled by avoiding temperature ranges that activate nucleation, a TS aging treatment was developed to enhance CFT.<sup>4</sup> The initial aging sequence (20 hr at 270 °F) promotes  $\theta''$  and  $T_1$  nucleation and growth in the matrix, while reducing  $T_1$  nucleation at subgrain boundaries (see fig. 10).  $T_1$  will eventually nucleate at subgrain boundaries and start to grow as aging continues (45 hr at 280 °F). However, the TS aging treatment allows  $T_1$  to precipitate and grow in the matrix before it can develop in the subgrain boundaries. The early coarsening of matrix  $T_1$  greatly reduces the concentration of Cu and Li in the matrix and thus hinders the growth of subgrain boundary  $T_1$  in a diluted Al-Cu-Li solid solution. The higher temperatures used in conventional aging (32 hr at 290 °F) are not encountered during TS aging, which helps to constrain  $T_1$  nucleation and growth at subgrain boundaries. As a result, a TS-aged specimen has a significantly different microstructure from that of a conventionally aged specimen (see fig. 11). Tests have indicated that TS aging can enhance CFT by as much as 30 percent (see fig. 12).

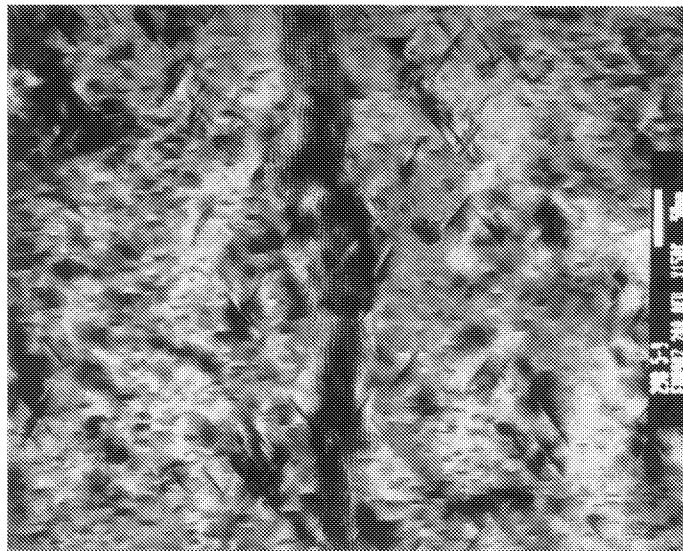


Figure 10. Enhanced  $\theta''$  and  $T_1$  nucleation in the matrix (rather than at subgrain boundaries) during the first step of TS aging (270 °F/20 hr).

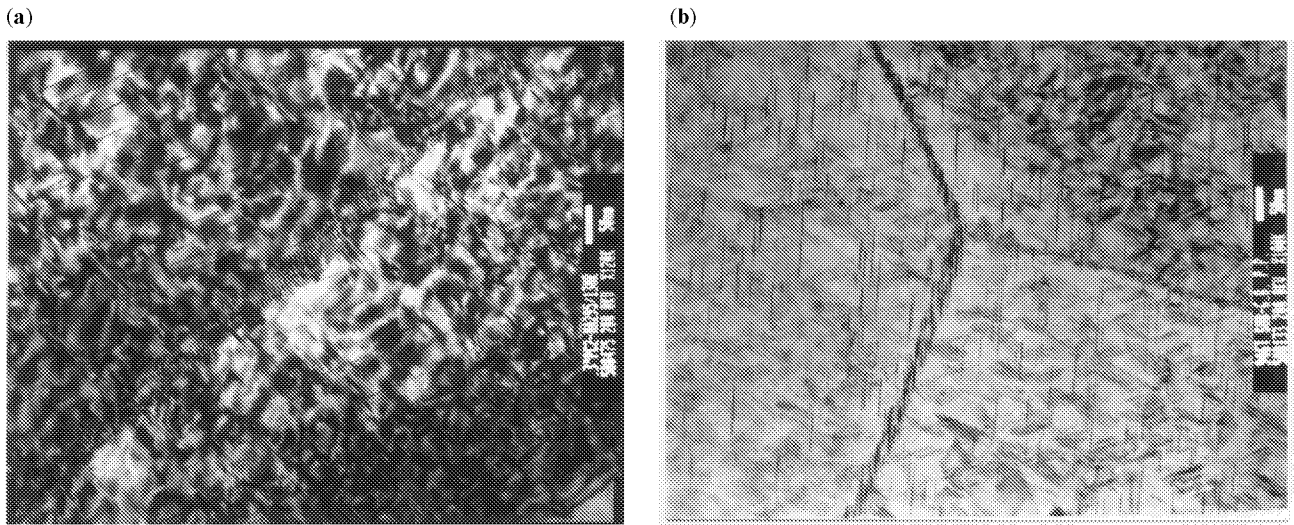


Figure 11. (a) No  $T_1$  precipitation seen at subgrain boundaries after TS aging as compared to (b) preferential  $T_1$  precipitation seen at subgrain boundaries after conventional aging.

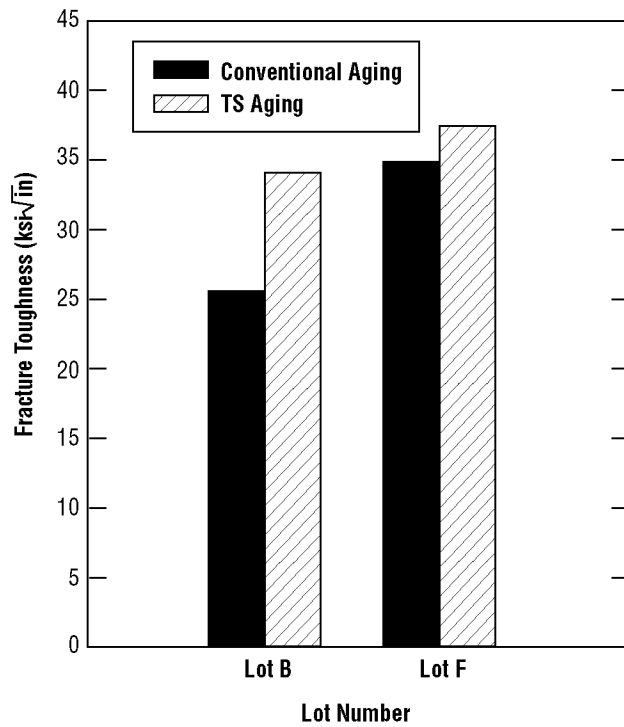


Figure 12. Significantly enhanced CFT of Al-Li 2195 after TS aging.

## 5. SUMMARY

1. TTP diagrams were determined for Al-Li 2195. They consisted of six separate C-curves for the matrix and four C-curves for the subgrain boundaries.
2.  $T_1$  was the primary strengthening phase at temperatures  $<500$  °F.
3. At temperatures  $<600$  °F,  $T_1$  was the only phase present at the subgrain boundaries. At temperatures between 300 and 500 °F, initial nucleation of  $T_1$  occurred preferentially at the subgrain boundaries, with more  $T_1$  growth seen there than in the matrix.
4. At temperatures  $>600$  °F,  $\theta'$ ,  $\theta$ ,  $T_2$ , and  $T_B$  formed at the subgrain boundaries and in the matrix. Prolonged exposure at 800 °F resulted in the precipitation of equilibrium phases  $T_B$  and  $T_2$ . Apparently,  $T_B$  grew at the expense of  $\theta'$  and  $\theta$ , whereas  $T_2$  coexisted with  $\theta$  at the grain boundaries (which led to continuous grain boundary coverage).
5. At temperatures  $>600$  °F, a significant drop in hardness occurred, which can be explained by insufficient nucleation of  $T_1$  and precipitation of incoherent equilibrium phases  $\theta$ ,  $T_B$ , and  $T_2$ . At temperatures  $>900$  °F, significant recrystallization and grain growth resulted in a microstructure that was essentially devoid of any strengthening precipitates.
6. This study developed TTP diagrams which were instrumental in the development of an advanced aging treatment for Al-Li 2195 that is now being used in the SLWT program. This aging treatment has proved to be capable of improving the size, distribution, and density of  $T_1$  in Al-Li 2195 and hence improving the alloy's CFT by up to 30 percent.

## REFERENCES

1. Chen, P.S.; and Stanton, W.P.: "A New Aging Treatment for Improving Cryogenic Toughness of the Main Structural Alloy of the Super Lightweight Tank," *NASA Technical Memorandum 108524*, 1996.
2. Chen, P.S.; Kuruvilla, A.K.; Malone, T.W.; and Stanton, W.P.: "The Effects of Artificial Aging on the Microstructure and Fracture Toughness of Al-Cu-Li Alloy 2195," *J. Mater. Eng. & Per.*, Vol. 7, p. 682, 1998.
3. Blankenship, Jr., C.P.; and Starke, Jr., E.A.: "Structure-Property Relationships in Al-Li-Cu-Mg-Ag-Zr Alloy X2095," *Acta. Metall.*, Vol. 42, p. 845, 1995.
4. Chen, P.S.; and Stanton, W.P.: "Artificial Aging Effects on Cryogenic Fracture Toughness of the Main Structural Alloy for the Super Lightweight Tank," *NASA Technical Memorandum*, publication pending, 2002.
5. Pickens, J.R.; Kumar, K.S.; Brown, S.A.; et al.: "Evaluation of the Microstructure of Al-Cu-Li-Ag-Mg Weldalite™ Alloys," *NASA Contractor Report 4368*, 1991.

REPORT DOCUMENTATION PAGE			Form Approved OMB No. 0704-0188	
Public reporting burden for this collection of information is estimated to average 1 hour per response, including the time for reviewing instructions, searching existing data sources, gathering and maintaining the data needed, and completing and reviewing the collection of information. Send comments regarding this burden estimate or any other aspect of this collection of information, including suggestions for reducing this burden, to Washington Headquarters Services, Directorate for Information Operation and Reports, 1215 Jefferson Davis Highway, Suite 1204, Arlington, VA 22202-4302, and to the Office of Management and Budget, Paperwork Reduction Project (0704-0188), Washington, DC 20503				
1. AGENCY USE ONLY (Leave Blank)	2. REPORT DATE February 2002	3. REPORT TYPE AND DATES COVERED Technical Memorandum		
4. TITLE AND SUBTITLE Time-Temperature-Precipitation Behavior in Al-Li Alloy 2195			5. FUNDING NUMBERS	
6. AUTHORS P.S. Chen* and B.N. Bhat				
7. PERFORMING ORGANIZATION NAMES(S) AND ADDRESS(ES) George C. Marshall Space Flight Center Marshall Space Flight Center, AL 35812			8. PERFORMING ORGANIZATION REPORT NUMBER  M-1043	
9. SPONSORING/MONITORING AGENCY NAME(S) AND ADDRESS(ES) National Aeronautics and Space Administration Washington, DC 20546-0001			10. SPONSORING/MONITORING AGENCY REPORT NUMBER  NASA/TM-2002-211548	
11. SUPPLEMENTARY NOTES Prepared for the Engineering Directorate, Materials, Processes, and Manufacturing Department * IIT Research Institute, Huntsville, AL				
12a. DISTRIBUTION/AVAILABILITY STATEMENT Unclassified-Unlimited Subject Category 26 Nonstandard Distribution			12b. DISTRIBUTION CODE	
13. ABSTRACT (Maximum 200 words)  Transmission electron microscopy was used to study time-temperature-precipitation (TTP) behavior in aluminum-lithium (Al-Li) 2195 alloy. Al-Li 2195 (nominally Al + 4 percent Cu + 1 percent Li + 0.3 percent Ag + 0.3 percent Mg + 0.1 percent Zr) was initially solutionized for 1 hr at 950 °F and then stretched 3 percent. Heat treatments were conducted for up to 100 hr at temperatures ranging from 200 to 1,000 °F. TTP diagrams were determined for both matrix and subgrain boundaries. Depending upon heat treatment conditions, precipitate phases (such as GP zone, $\theta''$ , $\theta'$ , $\theta$ , $\delta'$ , $T_1$ , $T_B$ , and $T_2$ ) were found in the alloy. The TTP diagrams were applied as a guide to avoid $T_1$ precipitation at subgrain boundaries, as part of an effort to improve the alloy's cryogenic fracture toughness (CFT). New understanding of TTP behavior was instrumental in the development of a two-step artificial aging treatment that significantly enhanced CFT in Al-Li 2195.				
14. SUBJECT TERMS Al-Cu-Li 2195, Al-Li 2195, time-temperature-precipitation (TTP) diagrams, microstructural characterization, cryogenic fracture toughness (CFT), two-step aging treatment, welding parameters			15. NUMBER OF PAGES 20	
			16. PRICE CODE	
17. SECURITY CLASSIFICATION OF REPORT Unclassified	18. SECURITY CLASSIFICATION OF THIS PAGE Unclassified	19. SECURITY CLASSIFICATION OF ABSTRACT Unclassified	20. LIMITATION OF ABSTRACT Unlimited	

National Aeronautics and  
Space Administration  
AD33

**George C. Marshall Space Flight Center**  
Marshall Space Flight Center, Alabama  
35812

